JOURNAL OF GEOPHYSICAL RESEARCH, VOL. 89, NO. A1, PAGES 301-315, JANUARY 1, 1984

THERMOSPHERIC CONTROL OF THE AURORAL SOURCE OF O^+ IONS FOR THE MAGNETOSPHERE

M Lockwood[1]

Radio Research Centre, Auckland University

Abstract. Linear theory, model ion-density profiles and MSIS neutral thermospheric predictions are used to investigate the stability of the auroral, topside ionosphere to oxygen cyclotron waves: variations of the critical height, above which the plasma is unstable, with field-aligned current, thermal ion density and exospheric temperature are considered. In addition, probabilities are assessed that interactions with neutral atomic gases prevent O^+ ions from escaping into the magnetosphere after they have been transversely accelerated by these waves. The two studies are combined to give a rough estimate of the total O^+ escape flux as a function of the field-aligned current density for an assumed rise in the perpendicular ion temperature. Charge exchange with neutral oxygen, not hydrogen, is shown to be the principle limitation to the escape of O^+ ions, which occurs when the waves are driven unstable down to low altitudes. It is found that the largest observed field-aligned current densities can heat a maximum of about 5×10^{14} O^+ ions m^{-2} to a threshold above which they are subsequently able to escape into the magnetosphere in the following 500s. Averaged over this period, this would constitute a flux of 10^{12} m^{-2} s^{-1} and in steady-state the peak outflow would then be limited to about 10^{13} m^{-2} s^{-1} by frictional drag on thermal O^+ at lower altitudes. Maximum escape is at low plasma density unless the O^+ scale height is very large. The outflow decreases with decreasing field-aligned current density and, to a lesser extent, with increasing exospheric temperature. Upward flowing ion events are evaluated as a source of O^+ ions for the magnetosphere and as an explanation of the observed solar cycle variation of ring current O^+ abundance.

1. Introduction

In recent years it has become apparent that the magnetosphere contains a substantial and variable O^+ component (see reviews by Horwitz [1982] and Hultqvist [1982a]). These ions are found over a wide range of energies throughout the magnetosphere: in the plasma sheet and lobes [Sharp et al., 1981], the ring current [Balsiger et al., 1980], the mantle [Lundin et al., 1982a], the magnetotail boundary layer [Candidi et al., 1982] and the sub-solar magnetopause, boundary layer and magnetosheath [Peterson et al., 1982]. Studies of the plasma in the ring current and plasma sheet have stressed the variability of the abundance of the O^+ ions; for example Peterson et al., [1981] observed O^+ to comprise between 2 and 70% of plasma sheet ions having an energy per charge of 10 eV/q to 17 keV/q. Circulation of heavy ions throughout the magnetosphere, owing to the convection electric field, was first suggested by Freeman et al., [1977]. The source of the magnetospheric O^+ is known to be the ionosphere because the solar wind contains practically no O^+ and only small numbers of O^{6+} [Bame et al., 1970]; the fluxes being insufficient to explain magnetospheric abundances even if efficient entry and charge exchange mechanisms are present [Prange, 1978; Johnson, 1979].

Upward-flowing ions (UFI's) of ionospheric origin are observed over a wide range of altitudes along auroral field lines [Ghielmetti et al., 1978]. The composition of UFI's varies from nearly pure O^+ to nearly pure H^+ [Kintner et al., 1979; Collin et al., 1981; Lundin et al., 1982b] and O^+ fluxes have been observed out to 35 R_E in the magnetotail [Frank et al., 1977; Formisano et al., 1981]. The pitch angle distributions are either conical (with a variety of cone angles between zero and 90°) or field-aligned (cone angle equals zero, to within angular resolution of detector). The morphologies of these conics and beams have been studied by Gorney et al., [1981]. Conics are observed in the topside ionosphere, with cone angles close to 90° and only small upward field-aligned velocity components [Klumpar, 1979; Ungstrup et al., 1979]. The pancake pitch angle distributions of these transversely-accelerated ions (TAI's) indicate that the observations are made above the region of transverse ion heating. Source heights for TAI's as low as 400 km have been observed by rocket observations [Yau et al., 1983].

For adiabatic, scatter-free motion, a TAI would evolve into a low-energy conic at greater altitudes; the peak of the pitch-angle distribution being folded to smaller cone angles by the divergence of the geomagnetic field. The fluxes of TAI's observed at 1400 km by the ISIS 2 ion mass spectrometer are greatest at the instrument's energy thereshold of 5 eV and are smaller by a factor of roughly 100 at the maximum observed energies of about 50 eV [Ungstrup et al., 1979]. Thermal plasma experiments on board ISEE 1 and DE 1 reveal that some ions reach greater altitudes with little further acceleration [Horwitz et al., 1982; Gurgiolo and Burch, 1982]. However, others are detected by S3-3 to have undergone additional heating: their energy is raised above the thresholds of the electrostatic analyser (90 eV, Gorney et al., [1981]) and even of the ion mass spectrometer (0.5 keV, Ghielmetti et al., [1978]). Comparison of the morphologies of the ions observed by these two experiments shows that

[1]Now at Rutherford Appleton Laboratory

Paper number 3A1269.
0148-0227/84/003A-1269$05.00

most of the heating to energies greater than 0.5 keV occurs above 5000 km [Gorney et al., 1981]. Oxygen ions in energetic UFI events are found to have slightly higher energies and broader pitch angle distributions than H^+ ions [Collin et al., 1981] implying the presence of additional transverse heating active only on the heavier ions. Moore [1980], Lockwood and Titheridge [1981] and Lockwood [1982] have argued that some such heating is required at ionospheric altitudes if O^+ ions are to escape into the magnetosphere, whereas sufficient thermal protons are supplied freely by the polar wind. Hultqvist [1982b] concludes from magnetospheric O^+ enhancements during storms, that heating must occur below 1000 km to give sufficient O^+ ions. Some observations have revealed such low-altitude O^+ acceleration, the lowest being at 600 km [Whalen et al., 1978]. Singh and Schunk [1982], by contrast, have recently suggested that the polar wind could contain significant O^+ by rapid ionospheric expansion; in which case O^+ could be supplied to the magnetosphere from the entire high-latitude region, not just the auroral oval. Pancake distributions of low energy O^+ (showing thermal plasma escape with subsequent local transverse heating) are rare in the magnetosphere, although the lowest energies may not have been sampled due to the spacecraft potential [Horwitz et al., 1981]. Recent results from the energetic ion composition spectrometer on DE1 confirm that significant O^+ can be added to the polar wind and that this species can dominate the low-energy ion outflow [Shelley et al., 1982].

Freeman et al., [1977] envisaged another alternative to auroral UFI events as a source of magnetospheric O^+: cold ions from the mid-latitude ionosphere accumulate in the outer plasmasphere and are subsequently detached into the plasma trough during periods of enhanced convection. However ISEE 1 observations of thermal plasma have shown that O^+ abundance within the plasmasphere is comparatively small: the transition to a region of larger (upward) fluxes of O^+ being coincident with the plasmapause, as seen in H^+ densities [Horwitz et al., 1981, 1982]. This is confirmed by initial results from DE 1, which detects some accumulation of thermal O^+ in the outer plasmasphere in a torus, but more O^+ flowing upward outside the plasmapause [Chappell, 1982]. In addition, the pitch angle and energy information from DE 1 reveals that at least a subset of past observations of detached plasma regions (for example by OGO 5) could have been UFI's from the ionosphere, in which case they were not plasmaspheric in origin [Chappell et al., 1982]. Within the plasmasphere the ions have isotropic, Maxwellian distributions ($kT < 1$ eV) and without any heating at low altitudes the O^+ component of the flow from the ionosphere should be small owing to charge exchange with hydrogen atoms [Moore, 1980; Lockwood, 1982]. Lockwood [1983] has shown that total ion outflow at mid-latitudes is indeed approximately equal to the expected thermal proton flux, at least under quiet geomagnetic conditions. Outside the plasmapause ions can have energies greater than 1 eV, to which they are limited inside the plasmasphere [Chappell, 1982]. If heating to greater than about 10 eV occurs at ionospheric altitudes, this is sufficient to allow O^+ to escape with significant steady-state fluxes. Hence the main source of magnetospheric O^+ may not be plasmaspheric, but due instead to upward flows outside the plasmasphere. The rapidity with which the dayside magnetosphere fills with O^+ during the onset of a storm led Hultqvist [1982a] to a similar conclusion.

Three years of ring current composition observations by GEOS 1 and 2 have revealed a solar cycle dependence of the O^+ ion abundance in the energy range 0.9-13.9 keV [Young et al., 1981, 1982]. Between 1977 and 1980 the ratio of the O^+ to H^+ number densities rose from 0.08 to 0.8, while the 10.7-cm solar flux rose from 75 to 200. Other ion ratios showed no such systematic change. SCATHA observations near geosynchronous orbit frequently reveal two contrasting ion populations in ion "zipper" events: high-energy pancake H^+ distributions, convected from the plasma sheet, are mixed with lower-energy field-aligned distributions, dominated by O^+ and believed to be injected directly from the ionosphere [Kaye et al., 1981]. Young et al. attribute the rise in the O^+/H^+ ratio to an increase in the numbers of O^+ of the field-aligned ion population, owing to the rise in topside O^+ densities. However, ISIS 2 observations show that the TAI events are less frequent when the topside O^+ density is high [Klumpar, 1981]. Hence, if TAI events are the source of the O^+ component of ion zipper events, the solar cycle dependence of the O^+/H^+ ratio is not due to modulation of this source by ionospheric O^+ densities. Lyons and Moore [1981] have suggested the differing rates for charge exchange of O^+ and H^+ with the geocoronal H may explain the high O^+/H^+ ratio for the ring current (compared with that of UFI events) and a solar-cycle dependence of these loss mechanisms is to be expected. Moore [1980] has noted that the neutral thermosphere also influences the source of the O^+.

In this paper the ionospheric source of O^+, via TAI events, is investigated and the expected variations with the neutral thermosphere and the F10.7 index is discussed. Variations of the transverse acceleration mechanism are studied in section 3, following a review of relevant theories and laboratory experiments in section 2. Sections 4 and 5 address the probability of an ionospheric O^+ ion escaping into the magnetosphere after it has been accelerated. The conclusions from these studies are combined in section 6 to give maximum estimates of O^+ escape, which are compared with experimental data in section 7.

2. Transverse Ion Heating in the Topside Ionosphere

The effects of a transverse acceleration mechanism are regularly observed in the topside auroral ionosphere: TAI events and their effects on thermal plasma dynamics are found with occurrence frequencies exceeding 0.4 in winter [Klumpar, 1979; Lockwood, 1982]. However, direct observations of the mechanism responsible have not been possible.

At great altitudes, proton conics have been observed in association with electrostatic ion cyclotron turbulence at frequencies close to the proton gyrofrequency [Kintner et al., 1979] and within regions of downward field-aligned current [Cattell, 1981]. These currents are predominantly carried by upward drifts of low-energy, ionospheric electrons and the critical drift required to excite the ion-cyclotron instability was studied by Kindel and Kennell [1971] by using linear theory, applied to the marginal stability condition. They found ion cyclotron waves to have the lowest of all the instability thresholds and predicted that both oxygen and hydrogen waves should be excited in the topside ionosphere by the observed field-aligned current densities.

Laboratory experiments on electron beam excitation of ion cyclotron waves in Q machines have shown that ion heating can result [e.g. Rynn et al., 1974; Dakin et al., 1976; Hauck et al., 1978] and that non-linear saturation occurs. Quasi-linear theories of heating by coherent ion cyclotron waves or by turbulence have been developed [Lysak et al., 1980; Dusenbery and Lyons, 1981] in which a limit to the transverse ion temperature, $T_{\perp i}$, is set by the formation of a plateau in the electron velocity distribution. The earlier theory of Dum and Dupree [1970] indicated that saturation may be due to the nonlinear phenomenum of resonance broadening, which is consistent with the results of some laboratory experiments [Bohmer and Fornaca, 1979]. Lee [1972] studied the dependence of the critical drift (required to destabilize ion cyclotron waves) on the ratio $T_{\parallel e}/T_{\perp i}$: if the anisotropy of the ion temperature is sufficiently large this ratio can fall below a threshold at which the instability shuts off. Some numerical simulations have reproduced this limitation to $T_{\perp i}$ [Ionson et al., 1979; Ashour-Abdalla et al., 1981]; whereas Hudson et al., [1978] predict $T_{\perp i}$ and $T_{\parallel e}$ to grow at similar rates and then saturation is by resonance broadening.

The uncertainty concerning the mechanism of nonlinear saturation means that the final transverse temperatures that the ions can achieve are not known in detail. In addition the Larmor radius may become comparable to the width of the channel carrying the destabilising field-aligned current. In such cases density depletions within the channel are observed in Q machines, owing to transport of heated ions perpendicular to the magnetic field [Stern et al., 1976]. The heated ions form an annulus around the channel [Bohmer and Fornaca, 1979] and their removal to a region stable to ion-cyclotron waves may limit the value of $T_{\perp i}$ before any of the saturation mechanisms becomes effective. Hudson et al. [1978] estimate that the Larmor radius is comparable in size to auroral field-aligned current channels for keV ions; such energies are achieved above about 5000 km [Gorney et al., 1981]. Hence in the topside ionosphere the lower temperatures of the ions indicate that they should remain within the region of heating until removed (upward) by the gradient-B, mirror force.

Because the ion-ion collision frequency is very low in regions of auroral transverse acceleration, Lysak et al., [1980] argue that a hot tail of the ion distribution should form and persist because thermalization by unheated ions is slow. However, laboratory experiments [Bohmer et al., 1978; Bohmer and Fornaca, 1979] and numerical simulations [Okuda and Ashour-Abdalla, 1981; Pritchett et al., 1981] designed to reproduce topside, auroral, ionospheric conditions have shown that the transverse ion-velocity distribution remains Maxwellian in form during ion cyclotron heating to within about 5%. As bulk heating occurs under these conditions, thermalization by turbulent wave-particle interactions must be efficient.

Kindel; and Kennel [1971] make approximate allowance for the effect of ion-neutral collisions on the marginal stability condition for ion-cyclotron wave growth. To date, nonlinear simulations of ion heating due to ion-cyclotron waves have not included ion-neutral collisions and these will introduce quenching of the heating [Yau et al., 1983]. The simulation by Ashour-Abdalla et al., [1981] shows that in the absence of neutral atoms $T_{\perp i}$ saturates 1500 ΩH^{-1}S. after the onset of ion heating. If this period is comparable or greater than the charge exchange collision period the heating will be quenched by energy transfer to the neutral gas.

Processes other than oxygen-cyclotron wave heating have been proposed for transverse acceleration of O^+ in the topside ionosphere: for example, stochastic acceleration by hydrogen cyclotron waves [Papadopoulos et al., 1980] or resonance with lower hybrid waves [Klumpar, 1979]. However, such processes are efficient only when O^+ is a minority constituent or when the O^+ ions are pre-heated by other means [Mozer et al., 1980]. Hence, as discussed by Lockwood [1982], these processes are unlikely to be responsible for the initial heating of thermal ionospheric O^+ and for escape of O^+ into the magnetosphere. From a model of rapid expansion of ionospheric plasma (for example, following density enhancements or flux tube configuration changes), Singh and Schunk [1982] find that accelerated O^+ may be added to the polar wind outflow of light ions. At present it is only possible to simulate behaviour for a small range of altitudes but if such a process is effective, it could act in any part of the polar cap and not just in auroral regions. In this paper only O^+ heating by oxygen cyclotron waves will be considered. Other heating processes may determine the ultimate $T_{\perp i}$ of the ions, and hence their destination within the magnetoshere [see Cowley, 1980; Candidi et al., 1982], but are not considered to be involved in their initial escape from the ionosphere.

3. Variations in the Stability of the Topside Ionosphere to O^+ Ion-Cyclotron Waves

The linear theory of Kindel and Kennel [1971], although unable to predict the rise in transverse ion temperature, does allow the identification of the conditions which may lead to such heating. In addition, approximate allowance for ion-neutral collisions can be made, which have not been included in any of the nonlinear simulations.

The marginal stability condition for a

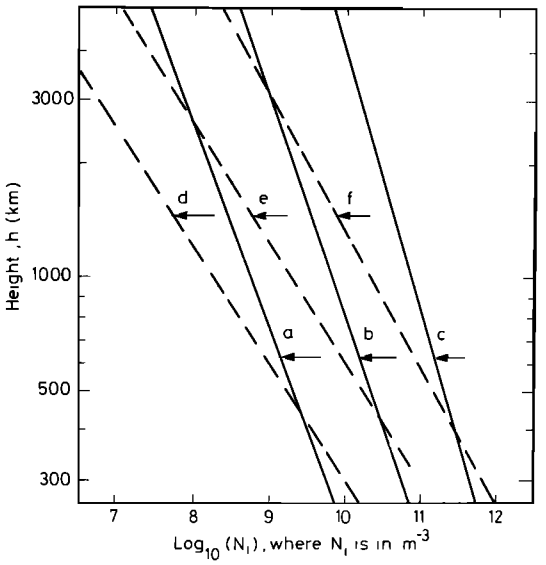

Fig. 1. Model O^+ density profiles.

single ion species, equation (21) of Kindel and Kennel, is evaluated here for six model profiles of the thermal O^+ ion density. The adopted profiles are all linear on logarithmic plots and are in pairs with equal densities at 400 km, $N_i(400)$ for low or high density gradients, dN_i/dh, (high or low O^+ scale height, H, respectively) as shown in Figure 1. The ratio of electron to ion temperatures is given a single model profile in all three cases, with a peak value of 1.6 at 400 km, decreasing to near unity by 700 km. Figure 2 shows the computed critical current densities required to drive ion cyclotron waves for pure O^+ plasmas of these density profiles. In all cases the critical current density (shown here normalized to 1400 km) increases with decreasing altitude and with increased plasma density. The approximate limit to the field-aligned current densities observed by the ISIS 2 spacecraft (at altitude $h_i \simeq 1400$ km) is shown as j_{max}. It can be seen that for case (e), the largest observed current densities drive some waves just below h_i, and if ion heating results, TAI events with pitch angle peaks close to 90° would be observed. For cases (a) and (d) TAI events would be expected for lower field-aligned current densities, but for cases (b), (c), and (f) the high ion density means that no TAI events would be observed. As discussed by Klumpar [1981], this behavior is qualitatively consistent with TAI occurrence morphology observed by ISIS 2; events being observed at high field-aligned current densities and low ion densities. Figure 3 plots the total content of the plasma column for which the ion cyclotron waves are unstable, N_T, as a function of field-aligned current density j for the model O^+ density profiles. The column therefore extends from the critical height, above which the topside ionosphere is unstable to ion cyclotron waves, to infinity. For the profiles of higher O^+ scale height (a, b, and c) N_T increases with $N_i(400)$ for the largest values of j. However, near j = 100 μA m^{-2} curve (c) falls below (b) and near j = 0.1 μA m^{-2} (b) falls below (a). Similar transitions occur for the low H cases, curves (d), (e) and (f), but at lower j. When H is large and for the expected range of j (< 10 μA m^{-2}), N_T generally decreases with $N_i(400)$; for the small H cases N_T also decreases with $N_i(400)$ at very small j (< 0.5 μA m^{-2}) but increases with $N_i(400)$ at j > 10 μA m^{-2}. This arises from two competing effects: an increase in $N_i(400)$ causes a rise in the critical height for the instability, h_c (Figure 2), which tends to reduce N_T; but also increases $N_i(h)$ for all h greater than h_c, thereby tending to increase N_T. When the O^+ density does not fall off rapidly (large H) the former effect dominates for the expected range of j.

Kindel and Kennel have shown that ion-neutral collisions tend to stabilise ion cyclotron waves. Hence enhanced neutral densities would raise the collision frequency and the critical current density required to drive the waves. Using the approximate equations given in appendix A of Kindel and Kennel this effect was evaluated by using the MSIS79 model of thermospheric densities [Hedin et al., 1979]. Figure 4 plots the results for local midnight in winter. The critical height, h_c, above which the waves are unstable to the field-aligned current, is shown as a function of the value when collisions are absent, $[h_c]_{\nu=0}$, for (a) F10.7 = 80 and (b) F10.7 = 230. In both cases a low Ap value of 2 was used, giving exospheric temperatures of 669K for (b) and 1080K for (a). It can be seen that ion-neutral collisions raise the critical height, although the effect is negligible above about 400 km for (a) and 600 km for (b). For summer conditions the effect is even smaller. Hence, although enhanced F10.7 flux does tend to stabilise ion-cyclotron waves, the effect at the altitudes of importance (above about 500 km) is very small and this mechanism would appear to not exert a

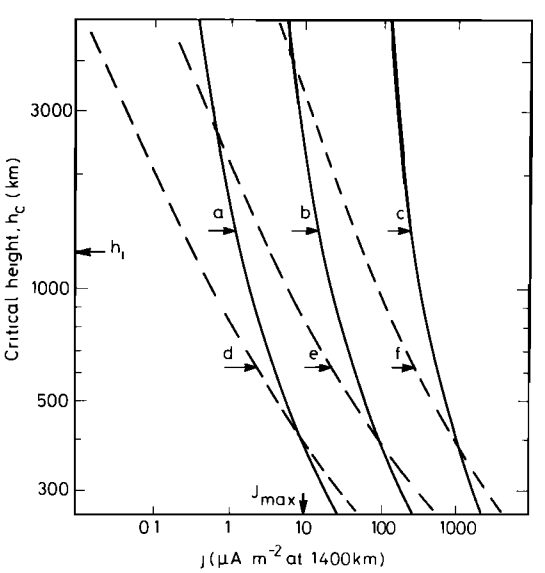

Fig. 2. Critical curent density profiles, $j_c(h)$, evaluated using the marginal stability condition by Kindel and Kennel [1971] for plasma density profiles given by Figure 1.

controlling influence on escape of O^+ ions by ion-cyclotron heating.

4. Interactions of an O^+ Conic With the Neutral Thermosphere

For the heights at which O^+ ions are transversely accelerated, neutral oxygen atoms may be an important (or even the dominant) thermospheric constituent. At greater heights, however, atomic hydrogen will dominate. For both of these neutral gases there are two types of interaction with the transversely-accelerated O^+ ion that may determine whether or not it escapes into the magnetosphere: ion-neutral charge exchange and elastic scatter of the ion. Energetic O^+ ions lose their energy to neutral O atoms via these two processes [Torr et al., 1974; Torr and Torr, 1979] :

Charge exchange $O_f^+ + O \rightarrow O_f + O^+$

Elastic scatter $O_f^+ + O \rightarrow O_f^+ + O_f$

where the subscript f is used to denote an energetic ion or atom.

In the charge exchange interaction, the incident ion strips an electron from the atom but loses very little energy to it; the products of the interaction are an energetic neutral atom and a cold ion. For the low energies of O^+ conics observed in the topside ionosphere, the atom produced by the interaction is not sufficiently energetic to produce an ion by collision with a thermal atom [Torr and Torr, 1979]. Torr and Torr estimate that only 0.6% of 6 eV O atoms formed at 600 km will photoionize and only 0.4% will charge exchange to give O^+ ions; for 10 eV atoms they estimate even fewer (0.3%) give escaping O^+ ions. Here these small fractions are neglected and it is assumed that the O atoms, once found, do not give O^+ ions by either the reverse charge exchange reaction with O; by charge exchange with H^+ or by photoionization.

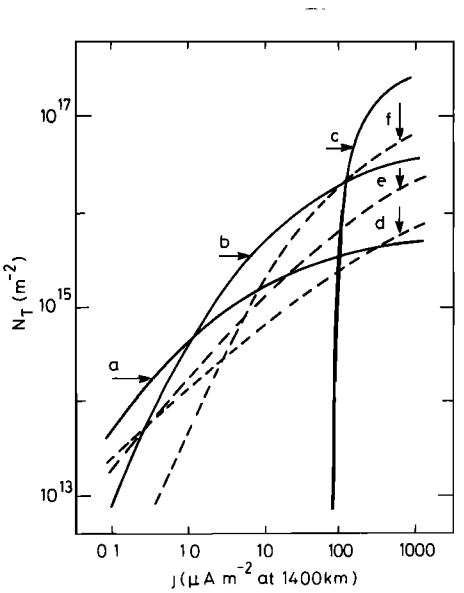

Fig. 3. Total O^+ content of column for which oxygen cyclotron waves are unstable N_T as a function of field-aligned current for plasma density profiles given by figure 1.

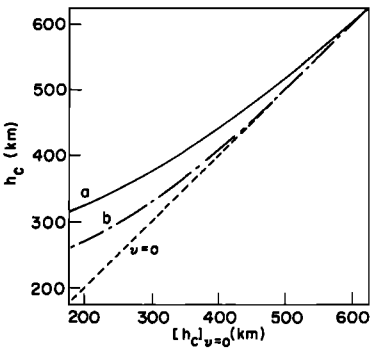

Fig. 4. Critical height, above which plasma is unstable to oxygen cyclotron waves, as a function of its value in the absence of ion-neutral collisions for MSIS79 predictions for geographic latitude of 54° and longitude of 60° at winter solstic with Ap of 2. (a) F10.7 = 80 (T_n = 699), (b) F10.7 = 230 (T_n = 1080).

If an ion (mass m_i) is scattered elastically by an atom of mass m_n, it will suffer a mean loss of energy per collision (in eV) of

$$\langle \Delta E_i \rangle = \frac{2\, m_i\, m_n}{(m_i + m_n)^2} \left(E_i - \frac{3\, kT_n}{2e} \right) \qquad (1)$$

4.1. Escape of an O^+ Ion to a Geocentric Distance r_t

Equation (A3) of appendix A shows that for an ion to escape adiabatically from r_o to r_t (where $v_{\parallel} = v_{\parallel t} > 0$) the initial transverse energy at r_o, $E_{\perp 0}$, must obey the inequality :

$$E_{\perp 0} \geq E_T = \left\{ E_e \left(1 - \frac{r_o}{r_t}\right) - E_{\parallel 0} \right\} / \left\{ 1 - \left(\frac{r_o}{r_t}\right)^3 \right\} \qquad (2)$$

where E_e is the gravitational escape energy to remove the ion to infinity, and is given by equation (A4).

Consider that the O^+ ion suffers a single collision at r_i during which it loses a fraction f of its energy ($f = \Delta E_i / E_i$) and is scattered to a pitch angle θ_i. The threshold for escape becomes

$$E_{\perp 0} \geq E_T' = \left[E_e \left\{ \frac{\left(\frac{r_o}{r_i} - \frac{r_o}{r_t}\right)}{(1 - f)\left\{1 - \sin^2\theta_i \left(\frac{r_i}{r_t}\right)^3\right\}} + 1 - \frac{r_o}{r_i} \right\} - E_{\parallel 0} \right] \Big/ \left[1 - \left(\frac{r_o}{r_t}\right)^3 \right] \qquad (3)$$

A single O^+-H charge exchange interaction will prevent the escape of the O^+ ion: an H^+ ion is produced, together with an O atom that is not sufficiently energetic to form a new O^+ ion (as assumed by Moore [1980]). Equation (3) demonstrates that a single O^+-O charge exchange will also prevent O^+ escape: for this inter-

action f is very close to unity as nearly all the energy of the incident ion is carried off by the neutral atom formed. Hence E_T' tends to infinity, and for the range of ion energies in the topside ionosphere, O^+ escape is not possible. The assumption that the energetic O atom produced is unable to produce an energetic O^+ ion at a later stage means that the apparent thickness of the barrier to O^+ escape may be overestimated and the probability of escape underestimated.

The fraction of the energy of the incident ion that is carried off by the ion following elastic scatter is given by (1). Neglecting the small energy of field-aligned motion prior to transverse heating ($E_{\parallel 0} \simeq 0$) and the thermal energy of the neutral atoms ($E_i >> 3kT_n/2$), equations (1), (2), and (3) show that a single scatter interaction raises the escape energy threshold by a factor β ($= E_T'/E_T$) which has a maximum value for $r_i = r_o$, given by

$$\beta_{max} = \frac{(m_i + m_n)^2}{(m_i^2 + m_n^2)} \left\{ \frac{(r_t/r_o)^3 - 1}{(r_t/r_o)^3 - \sin^2 \theta_i} \right\} \quad (4)$$

If the initial energy $E_{\perp 0}$ exceeds (βE_T), the ion will still always escape if $v_\parallel$ remains positive (upward) after scattering. Escape can still be possible if $v_\parallel$ becomes negative as the ion can mirror below r_c; alternatively, it may be scattered into a loss cone. If the heating, for example, occurs 600 km above the earth's surface, then the average β_{max} for escape to $r_t = 2R_E$ is 1.82 for scatter by O and 1.02 for scatter by H; hence in excess of two scatter interactions with O or 35 with H are required to make $E_{\perp 0}$ of 12 eV insufficient to cause any O^+ escape.

4.2. Cross Sections for the Various Ion Neutral Interactions

Consider an O^+ conic is given an initial energy $E_{\perp 0}$, which is equal to the threshold for escape to r_o (as given by equation 2). At r_t such an ion will have lost all its additional kinetic energy and will become part of a thermal, isotropic distribution. Hence it is necessary to consider the variation of the cross sections for the various interactions for ion energies between $E_{\perp 0}$ and thermal.

For energies below 500 eV ion-neutral charge exchange cross section can be expressed as [Banks, 1966] :

$$\sigma_c = (A - B \log_{10} \xi)^2 \quad (5)$$

where ξ is the kinetic energy of the relative motion (in eV) and A and B are constants. For a known neutral temperature and ion energy an rms value for ξ can be calculated by using equation (B3) of appendix B. For O^+-O charge exchange the low-energy values for A and B by Knof et al. [1964] are employed, namely, A of 5.59×10^{-10} m and B of 0.475×10^{-10} m. For O^+-H charge exchange the value for A is 3.47×10^{-10} m and that for B is 0.20×10^{-10} m [Banks and Kockarts, 1973]. For thermal ions (temperature T_i) in an atomic gas of the same species (temperature T_n), equation (5) gives a mean charge exchange cross section [Banks, 1966] :

$$\langle \sigma_c \rangle = \{(A + 3.96B) - B \log_{10} (T_i + T_n)\}^2 \quad (6)$$

For O^+ ions in a gas of H the mean cross section is [Banks and Kockarts, 1973]

$$\langle \sigma_c \rangle = \{4.26 - 0.2 \log_{10} T_i\}^2 . 10^{-20} \quad (m^2) \quad (7)$$

The velocity-dependent elastic scatter cross section is given by [Banks, 1966] :

$$\sigma_D = 6.582 \times 10^5 \left(\frac{a}{\mu}\right)^{1/2} \left(\frac{e}{\delta}\right) \quad (m^2) \quad (8)$$

where μ is the reduced mass, e is the electronic charge, δ is the relative ion-neutral velocity, and a is the polarizability of the neutral atomic gas. For O atoms a equals 0.79×10^{-30} m^3, for H it is 0.67×10^{-30} m^3 [Banks and Kockarts, 1973]. For thermal ions, (8) gives a mean cross-section of

$$\langle \sigma_D \rangle = 13.3 \times 10^{-3} \left(\frac{a}{\mu}\right)^{1/2} \left\{\frac{T_i}{m_i} + \frac{T_n}{m_n}\right\}^{-1/2} \quad (m^2) \quad (9)$$

The elastic scatter cross sections (σ_{DO}, σ_{DH} for scatter by O and H, respectively) and the charge exchange cross sections (σ_{cO} and σ_{cH}, respectively) calculated from equations (5) to (9) are listed in Table 1. The values are at various heights for an O^+ ion, which is initially heated to 12 eV above the mean thermal energy at a height of 600 km. The ion energy changes with height according to (A3) of Appendix A, and the neutral temperature is 1000K. The thermal ion cross sections are evaluated for T_i = 2500K (note that a 12-eV ion is never reduced to the mean thermal energy in travelling a finite distance from 600 km).

For the O^+-O interactions the charge exchange cross section is larger than that for elastic scatter at all heights. In addition, as was discussed in the previous section, only one such charge exchange reaction is required to prevent the O^+ escaping, whereas more O^+-O elastic scatter interactions would be required on average. It follows that the limit to O^+ escape placed by the presence of O is via charge exchange.

In contrast, the O^+-H elastic scatter cross section is always larger than that for O^+-H charge exchange. However, as was shown in the previous section, the O^+ ion must be scattered many times (in excess of 35) by H atoms for $E_{\perp o}$ to be insufficient for escape. Hence for scatter to be as important a barrier to the O^+ as is presented by charge exchange with H, the cross section must be larger by a factor of at least 35. Table 1 indicates that this is not the case, and charge exchange is the relevant interaction with H, as it is with O.

5. Results of Model Calculations for the Barrier Thickness, C

The effective thicknesses of the barriers to O^+ escape presented by charge exchange with O

TABLE 1. Charge Exchange and Elastic Scatter Cross Sections for O^+ Interactions With O and H (σ_{CO}, σ_{CH}, σ_{DO} and σ_{DH}, Respectively) for an O^+ Ion Heated by 12 eV at a Height of 600 km

Geocentric distance, r (R_E)	Ion Energy, E_i (eV)	Cross Sections (10^{-19} m^2)			
		σ_{CO}	σ_{CH}	σ_{DO}	σ_{DH}
1.1	12.0	2.72	1.22	0.67	1.68
1.5	9.5	2.77	1.23	0.75	1.85
2.3	7.0	2.84	1.24	0.88	2.07
∞	2.5	3.06	1.28	1.44	2.94
-	$\langle E_i \rangle = \frac{3}{2} k T_i$	3.35	1.28	2.83	3.30

T_n = 1000K, T_i = 2500K.

and H atoms (C, as defined by (B4)) were calculated by using (B5) for a variety of model thermospheric profiles. In all cases the profiles were for midnight at summer or winter solstice and a geographic latitude of 54° and longitude of 60° were obtained by using the MSIS79 model.

Figure 5 shows the variation of C with $E_{\perp O}$, the initial transverse energy imparted to the ion at a height of 600 km. A low Ap value of 2 was used for winter conditions with F10.7 of 200, giving an exospheric temperature of 1004K. Results are shown for escape to 2 R_E, 9 R_E, and infinity. If the initial energy does not exceed the gravitational escape energy required to reach these distances, C is infinite. However, above this threshold C is approximately independent of $E_{\perp O}$. In the following plots of this section $E_{\perp O}$ of 12 eV is considered which is sufficient to cause escape of an ion from 600 km to any altitude. In Figure 5, C is below unity when $E_{\perp O}$ = 12 eV for charge exchange by either O and H. Hence neither of these neutral gases prevent all escape of O^+; C for charge exchange with O is greater than that for H, hence in this example the former is the more effective in preventing escape of the O^+ ion.

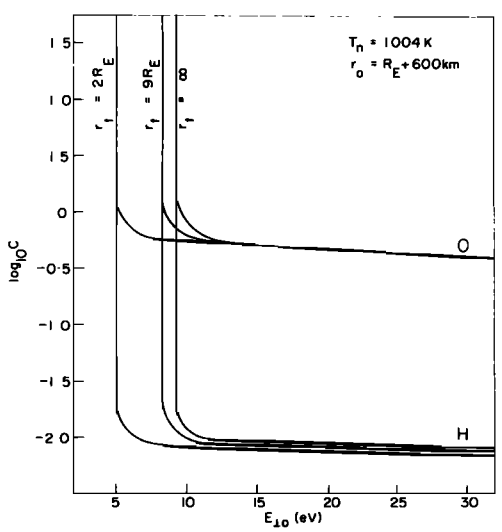

Fig. 5. Logarithm of thickness parameter C as a funtion of initial ion energy $E_{\perp O}$. Heating occurs at an altitude of 600 km and escape to $2R_E$, $9R_E$, and infinity is considered; the exospheric temperature is 1004K.

The variations of C with the altitude at which the ions are heated are plotted in Figure 6. Results are given for (1) the winter and (2) the summer solstices with three values for the 10.7-cm solar flux in each case; $E_{\perp O}$ is 12 eV and r_t is 2 R_E. At the lowest heating altitudes (< 500 km above the Earth's surface) O atoms always present a larger barrier to O^+ escape than do H atoms (larger C). Owing to the factor of 16 difference between the scale heights of these two neutral gases, the opposite is true above a transition altitude (marked by dots in Figure 6) which increases with F10.7 and T_n. For the oxygen case C is larger, for all source heights, when F10.7 is high, the converse being true for the hydrogen case. Hence the efficiency of the O barrier increases with F10.7, but that of the H decreases. Above the transition neither O nor H are particularly effective barriers (C < 0.1). In all cases the minimum height for ion escape (below which C > 1.0) is set by charge exchange with O.

Figure 7 shows variations of the source heights by giving two thresholds of C (1.0 and 0.1) with the exospheric temperature. For both summer and winter cases the expected range of exospheric temperatures causes an increase of

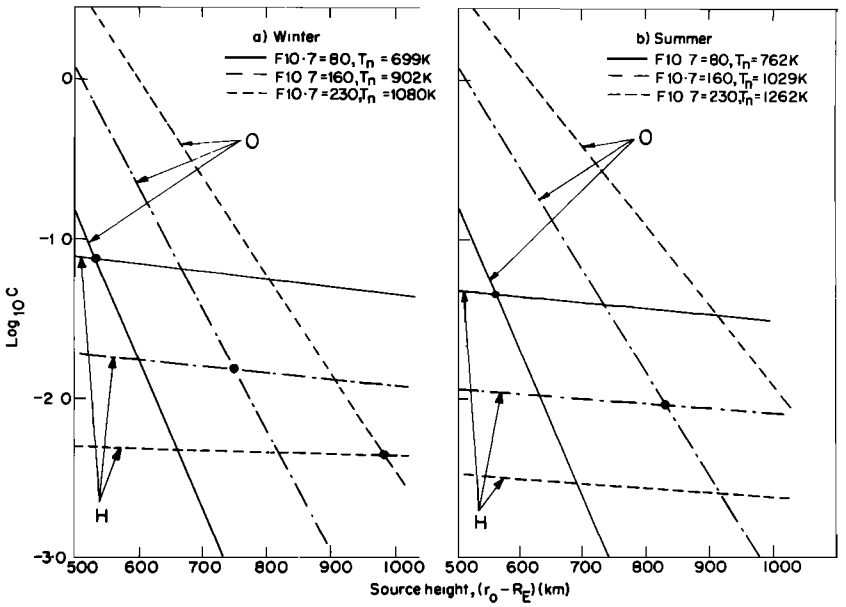

Fig. 6. Logarithm of thickness parameter C as a function of altitude of heating for (a) winter and (b) summer and three F10.7 values with Ap of 2 and $E_{\perp 0}$ of 12 eV. Results are shown for charge exchange with hydrogen (marked H) and oxygen (O) gasses.

about 200 km in the minimum source height from which O^+ ions can escape.

6. Model Calculations of Maximum O^+ Ion Escape Flux

By making some simplifying assumptions concerning the nature of the ion heating process, the results of the previous section can be used to estimate total O^+ escape fluxes from the auroral ionosphere, due to ion cyclotron heating, and their variations with F10.7.

Firstly it is assumed that oxygen cyclotron waves transversely accelerate ions at all altitudes down to the critical height, $r_c = h_c + R_E$, below which the instability shuts off. It is also assumed that during heating the distributions of both field-aligned and field-perpendicular ion velocities remain Maxwellian; $T_{\perp i}$ is raised by a factor that is assumed independent of height above the critical height, and $T_{\parallel i}$ is unaltered. The rationale for this assumption was discussed in section 2.

The probability p of an ion reaching a geocentric height r_t, after heating at r_o, is taken to be zero if C exceeds unity and is taken to be (1-C) at all lower C. Both C and p are assumed to be independent of the initial ion energy $E_{\perp 0}$ provided it exceeds the threshold for escape E_T given by (2). Figure 5 demonstrates that this is a valid approximation.

Consider the column of plasma in the flux tube between r_c and r_t, which has been heated to the saturation temperature $T_{\perp i}$. If at a time t = 0 the heating ceases at all altitudes, a total of S_e O^+ ions will be left in the column that are able to escape through the top of the column (i.e., for sufficiently high r_t, into the magnetosphere). By integrating over all source heights and all energies above the escape threshold E_T:

$$S_e = \int_{r_{c(j)}}^{r_t} p(r_o) \cdot N_i(r_o) \int_{E_{T(r_o)}}^{\infty} f(E_{\perp o}) dE_{\perp o} dr_o \qquad (10)$$

The ion density profiles at time t = 0, $N_i(r_o)$, defined by Figure 1, are again employed. Ashour-Abdalla et al. [1981] found that saturation of $T_{\perp i}$ occurred 1500 Ω_H^{-1}s. after the onset of heating, where Ω_H is the hydrogen gyrofrequency. This period is of the order of seconds in the topside ionosphere, during which the most energetic O^+ ions will have moved considerable distances. This makes

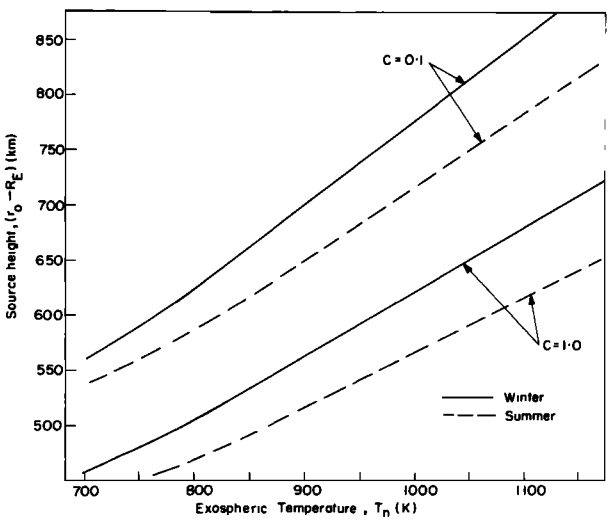

Fig. 7. Source height for which C equals 0.1 and 1.0 at $2R_E$ as a function of exospheric temperature for summer and winter, and $E_{\perp 0}$ of 12 eV.

the use of the simple profiles shown in Figure 1 for t = 0 a major simplification; however, for the want of more appropriate profiles, they do allow a first investigation of how S_e varies with ionospheric density. In all subsequent calculations a value of 2 R_E is adopted for r_t; results for greater r_t (9 R_E) are generally similar, however, the magnetic field model used is not appropriate for such great distances and motion may not remain adiabatic [Gorney et al., 1981].

The values of r_c corresponding to a given field-aligned current density j are scaled from figure 2 for each case. The distribution function $f(E_{\perp o})$ is assumed Maxwellian in form, with various values for the saturation transverse temperature $T_{\perp i}$ as a ratio of the unheated, isotropic value T_i (= 2500K) in the range 3-18. Ashour-Abdalla et al. [1981] obtained values of 6 and above for this ratio, depending on the field-aligned current. The probability p is computed from C, calculated by integration for each r_o with various model neutral atmospheric profiles (as described in sections 4 and 5).

Figure 8 shows the variation of computed values for S_e as a function of the ratio $(T_{\perp i}/T_i)$. It can be seen S_e falls off rapidly at $(T_{\perp i}/T_i)$ below about 5, but saturates at higher values. The examples given are for winter solstice profiles of thermospheric densities with exospheric temperatures of 700K, 900K, and 1100K; the field-aligned current density is 10 μA m^{-2} at 1400 km (near the maximum observed by ISIS 2) and N_i is described by the low-density profiles (a) and (d). The largest values of S_e are for the highest $T_{\perp i}$ and the lowest exospheric temperature and is of the order 5 x 10^{14} m^{-2}.

At a time t = 0, the first of these S_e ions will escape (those from $r_o = r_t$), the last to

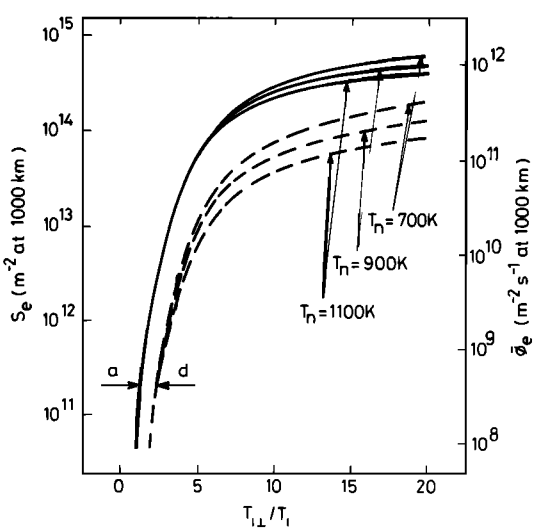

Fig. 8. Total number of ions escaping after removal of heating S_e as a function of the rise in perpendicular ion temperature $(T_{\perp i}/T_i)$ for three exospheric temperatures in winter and the depleted ion density profiles (a) and (d). The right-hand scale gives the mean flux $\langle\phi_e\rangle$ during the subsequent period of escape.

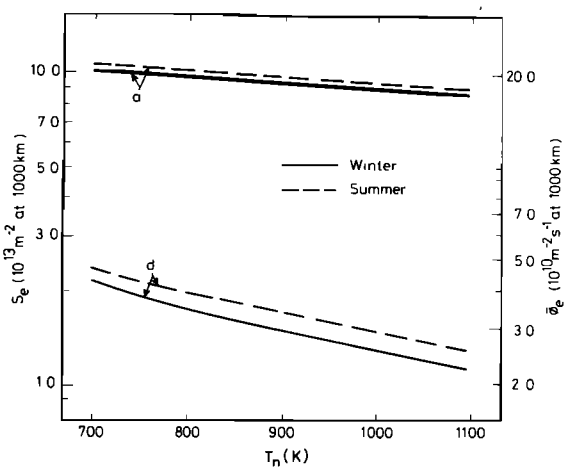

Fig. 9. Number of ions escaping after removal of heating S_e as a function of exospheric temperature for summer and winter with (a) high and (d) low O^+ scale - height profiles. The field-aligned current is 10μAm^{-2} at 1400km and $(T_{\perp i}/T_i)$ equals 6. The right hand scale gives the mean flux, $\langle\phi_e\rangle$, during the subsequent period of escape.

escape are those heated at $r_o = r_c$, to just above the threshold, $E_T(r_c)$. The latter ions reach r_t at a time t_1, from equation (A3) equal to 500s. for profiles (a) and (d) when j equals 10 μA m^{-2} (in both cases h_c = 400 km, Figure 2). The escape flux of O^+ ions, averaged over this period $\langle\phi_e\rangle$ is equal to (S_e/t_1). Equivalent values of $\langle\phi_e\rangle$ are given by the left hand scale of Figure 8, using the transit time t_1 computed from equation (A3). The escape flux at any time $\phi_e(t)$ will be smaller than $\langle\phi_e\rangle$ for t near 0 and will consequently be larger at some later times. Figure 8 shows that $\langle\phi_e\rangle$ easily exceeds 10^{10} $m^{-2}s^{-1}$ at $(T_{\perp i}/T_i)$ greater than about 4 for profile (a) and 5 for (d), independent of exospheric temperature.

In subsequent plots a value of $(T_{\perp i}/T_i)$ of 6 is employed, as modelled by Ashour-Abdalla et al. [1981] for the ion transition height. Figure 8 shows that higher values for this ratio give larger S_e and $\langle\phi_e\rangle$.

Figure 9 shows the variation of S_e with exospheric temperature for summer and winter with model ion density profiles (a) and (d). These values represent estimates of the maximum escape, due to the adoption of a maximum for the field-aligned current density of 10μA m^{-2} at 1400 km. For the large H profile (a), S_e is much the larger and is virtually independent of T_n. For the profile (d) the escape is smaller and, in addition, decreases with increased exospheric temperature. For the higher $N_i(400)$ profiles, (b) and (e), S_e is independent of T_n (owing to the high r_c values for even large j, the neutral themophere exerts no control on S_e) and equal to 6 x $10^{14}m^{-2}$ and $10^{13}m^{-2}$ respectively. Hence for the high H cases (a) and (b) S_e increases with $N_i(400)$ and for the low H cases S_e decreases slightly with $N_i(400)$, mainly due to the behavior of N_T, as discussed in section 3. When $N_i(400)$ is very large and H is high (profile c), S_e tends to zero owing to

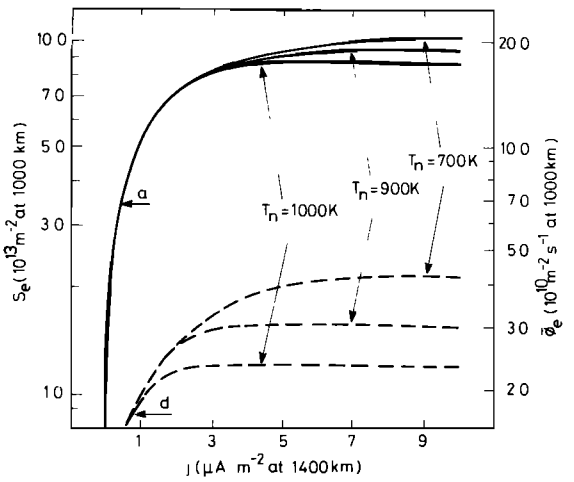

Fig. 10. Number of ions escaping after the removal of heating, S_e, as a function of field-aligned current j for (a) high and (d) low O^+ scale height profiles, winter conditions and exospheric temperatures of 700, 900 and 1100K. The right hand scale gives the mean flux $\langle\phi_e\rangle$ during the subsequent period of escape.

the small N_T for j = 10 μA m^{-2} (Figure 3).

The variation of S_e and $\langle\phi_e\rangle$ with the field-aligned current density is shown in Figure 10 for the ion density profiles (a) and (d). At low densities of field-aligned current, S_e is independent of T_n, owing to the large values of r_c. As the current density rises r_c decreases, giving an increase in S_e until r_c falls below the level for which C is unity and there is no further rise in S_e. Hence S_e and $\langle\phi_e\rangle$ are independent of the field-aligned current density at the largest observed values but are dependent on T_n.

The results for S_e and $\langle\phi_e\rangle$ depend sensitively on the critical height r_c. As r_c values are taken from the theory of Kindel and Kennel, all the results presented here are strongly dependent on the predictions of this theory.

7. Discussion and Comparison With Observed O^+ Escape Fluxes

Any O^+ ions lost to the magnetosphere from the plasma column between r_c and r_t would be replenished by upward flows of thermal O^+ through the base of the column. In steady state such flows are restricted to a limiting flux ϕ_L by frictional drag neutral atomic oxygen gas [Lockwood and Titheridge, 1982]. From topside soundings, Lockwood [1982] found mean values for ϕ_L in the auroral and polar regions of order 10^{13} m^{-2} s^{-1}, (normalized to 1000 km) with a maximum of about 5 x 10^{13} m^{-2} s^{-1}, near local midnight and at high Kp. If ϕ_L is much less than ϕ_e the limit to the O^+ escape flux in steady state would be set by the frictional drag and the escape flows would equal ϕ_L. Conversely, if ϕ_L is much larger than ϕ_e the limit is set by the ion heating process, all ions lost from the column would be replenished in steady state by the thermal ion flows at r_c.

Comparison of the values $\langle\phi_e\rangle$ given in the previous section (remembering that ϕ_e can exceed $\langle\phi_e\rangle$) with an order of magnitude estimate for ϕ_L of 10^{13} m^{-2} s^{-1} shows that the maximum, limiting outflow could be maintained in steady state if the field-aligned current is high, the ion heating is by a large factor ($T_{\|i}/T_i$ is large), and the exospheric temperature is low. If the field-aligned current is reduced, at some point ϕ_e will fall to ϕ_L; any further reduction would then cause a fall in the steady-state O^+ escape flux. For the high field-aligned current density of over 10 μA m^{-2} all six profiles shown in Figure 1 would give escape fluxes exceeding the 10^{13} m^{-2} s^{-2} limit. Generally, fluxes will be reduced at low $N_i(400)$ when H is large and at large $N_i(400)$ when H is small.

The fluxes of O^+ ions observed in the magnetotail by Frank et al. [1977] indicate a flux of about 10^{12} O^+ ions m^{-2} s^{-1} leaving the topside auroral ionosphere. This figure represents an integral over all pitch angles and the energy range of the IMP 7 electrostatic analyzer (50 eV-45 keV) and hence may be a slight underestimate, owing to ions outside this range. This escape flux is of the same order of magnitude as that for TAI events observed in the topside ionosphere by the ISIS 2 ion mass spectrometer [Klumpar, 1979; 1981; Ungstrup et al., 1979]. The relatively high energy thresholds for the electrostatic analyzer and ion mass spectrometer on board S3-3 mean that integrated O^+ ion flows in UFI events are likely to be underestimates as low energies (where O^+ abundances are highest [Lundin et al., 1982b] are not sampled. Spacecraft potentials may mean that this is also true, to a much lesser extent, of UFI data from low-threshold experiments like the plasma composition experiment (PCE) on board ISEE 1 and the retarding ion mass spectrometer (RIMS) on DE. None of the authors of the publications on DE, ISEE 1, or S3-3 data quote the required ionospheric O^+ escape flux; however, they do not state any disagreement with the initial estimate of 10^{12} m^{-2} s^{-1} by Frank et al., [1977]. Hultqvist [1982a;b] (see also Lundin et al. [1982a]) has argued that O^+ fluxes of this magnitude are required over a broad range of latitudes during magnetic storms, in order to explain observations of magnetospheric O^+ abundances.

The highest estimate for the O^+ escape flux, to date, has been given by Lundin et al. [1982b]. Using data from the ion composition spectrometers (ICS) on PROGNOZ 7 (0.2-17 keV), they find UFI events above 20000 km are consistent with an O^+ of up to 10^{13} m^{-2} s^{-1} for a source region at 500 km, or 5 x 10^{12} m^{-2} s^{-1} for a source region at 1500 km, if sufficient O^+ exists at such altitudes. Furthermore, the O^+ UFI events have very large latitudinal widths (typically 10°, as compared with the maximum of 8° observed by Ghielmetti et al. [1978] using S3-3) and Lundin et al. estimate that up to 2 x 10^{26} O^+ ions may be donated from the auroral oval to the magnetosphere, per second. In order to explain PROGNOZ 7 observations during the onset of a storm, Hultqvist

[1982b] has estimated that 10^{16} O^+ ions m^{-2} are fed into dayside magnetospheric flux tubes of a wide range of L. Such numbers of ions are only available if the heating mechanism extends down to very low altitudes (below 1000 km). This injection is suffient to make O^+ the dominant constituent of the entire dayside magnetosphere (in quiet periods O^+ only dominates in the near-earth region). The injection seems to be too rapid to permit convection to move O^+ from a localised source. If the factor of 10 rise in O^+ densities is achieved in a period of an hour or less, ion fluxes exceeding 3 x 10^{12} m^{-2} s^{-1} are required.

The mean escape fluxes modelled in the previous section $\langle\phi_e\rangle$ can achieve such high values under special sets of circumstances. Figure 8 shows that both profiles (a) and (d) allow fluxes of 10^{12} m^{-2} s^{-1} (at 1000 km) if $T_{\|i}/T_i$ exceeds 5. Figure 10 shows that the field-aligned current density need not be very large (of order 1 μA m^{-2} at 1400 km) and the exospheric temperature should be low (Figure 9). For the smallest current densities N_T and hence S_e and $\langle\phi_e\rangle$, are largest when the ionospheric density is low. Low exospheric temperatures and ion densities are most often found at sunspot minimum, when the occurrence of sufficiently large field-aligned currents is lower.

The possibility of such large O^+ escape flows has great implications for the dynamics of the thermal plasma of the topside ionosphere. Lockwood and Titheridge [1981] have detected large upward flows of thermal O^+ at low altitudes near the poleward edge of the auroral oval. Lockwood [1982] has shown that the occurrence morphology of events of large thermal O^+ flow is very similar to that of both UFI and TAI events and discussed possible connections between them. Observed thermal O^+ flows can be in excess of 10^{13} m^{-2} s^{-1}, but these would only equal the escape flux for steady-state conditions; an unknown fraction of this flux may contribute to refilling of the topside ionosphere. Large flux events were mainly observed at low topside ion densities and low exospheric temperatures; consistent with the occurrence of transverse acceleration-induced escape discussed in this paper for low field-aligned current densities. The dependence on the neutral thermosphere is confirmed by Figure 11 which shows the probability of observing a large thermal-ion flow event in a satellite pass through the auroral oval for the same database as used by Lockwood [1982], O^+ ion fluxes being computed by the procedure given by Lockwood [1983]. The probability is very high (about 0.75) at the lowest exospheric temperatures (below 700K) but falls off very rapidly at values near 800K.

Young et al., [1982] have found, from the GEOS data, that the number of 0.9 - 15.9 keV/e O^+ ions in the ring current obey the multiple regression equation

$$N(O^+) = (1.1 \times 10^4)\exp\{0.24\ Kp + 0.011\ \langle F10.7\rangle\} \pm (1.6 \times 10^5)\ m^{-3} \quad (11)$$

Hence their analysis reveals that, at a fixed mean F10.7, there is a strong enhancement

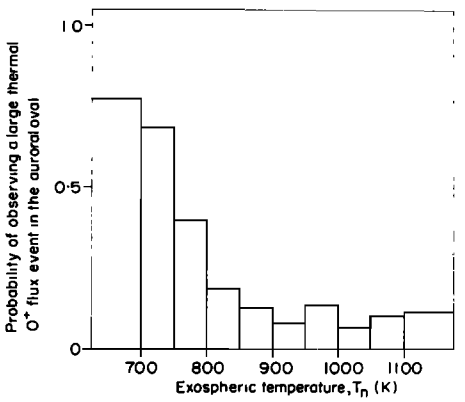

Fig. 11. Probability of a large thermal O^+ flux event in the auroral oval for the data set used by Lockwood [1982] as a function of exospheric temperature T_n.

of $N(O^+)$ with increased magnetic activity. Given that enhanced Kp is indicative of high field-aligned currents, the dependence of $\langle\phi_e\rangle$ on j (as modelled in section 6) is quantitatively consistent with the major O^+ escape mechnism being due to transverse ion acceleration at low altitudes. The variation of the ring current O^+ densities with the solar cycle, as found by Young et al., cannot so easily be attributed to modulation of these escape fluxes. The effect of charge exchange with the neutral thermosphere (as suggested by Moore [1980]) is mainly due to atomic oxygen and $\langle\phi_e\rangle$ decreases when F10.7, and hence the exospheric temperature is high. Hence this effect would tend to reduce O^+ densities in the magnetosphere at sunspot maximum, the opposite sense to the effect shown in (11). Young et al. [1982] attribute the higher O^+ numbers in the ring current to higher ionospheric densities. The results of the preceeding section show that $\langle\phi_e\rangle$ is only increased if the scale height of the O^+ ion distribution H is large. At 1000 km profiles (a), (b), and (c) have H of order 600 km, whereas for (d), (e), and (f) H is of order 300 km. Only for the higher H cases is it true that $\langle\phi_e\rangle$ increases with ionosheric density. The TAI events nearly all occur at latitudes where thermal plasma is streaming upward in the polar wind, which tends to increase H. Nevertheless, the topside soundings in the database used by Lockwood and Titheridge [1982] in general give H values nearer 300 km than 600 km for polar wind profiles (where the ion transition height is large) for solar minimum and the rising phase of the solar cycle. Under these conditions $\langle\phi_e\rangle$ falls with ionospheric density. Hence in order that high ionospheric densities give the high ring current densities at solar maximum a considerable increase in H is also required.

Alternatively, the solar cycle effect in ring current composition could be due to one of more of a number of competing processes; for example, scattering of UFI O^+ ions out of the loss core to give tapping, charge exchange of the trapped ions with geocoronal H (as suggested by Lyons and Moore [1981], or the higher

occurrence frequency at sunspot maximum of high-density field-aligned currents at a given Kp level. Other mechanisms for escape of O^+ ions may also explain the equation (11), for example via the plasmasphere (as suggested by Balsiger et al. [1980]) or rapid time-dependent polar wind expansion [Singh and Schunk, 1982].

8. Conclusions

Ion-neutral collisions tend to stabilize oxygen cyclotron waves in the topside ionosphere and hence raise the critical height down to which the waves are driven by a fixed field-aligned current density. However, MSIS neutral density predictions show that the effect is very small above about 500 km; hence this mechanism should not exert a controlling influence on the flow of transversely accelerated O^+ ions into the magnetosphere. The neutral thermosphere does, however, have an effect on the escape of the heated O^+ ions via charge exchange with neutral gases. For heating at lower altitudes (below 600-1000 km) charge exchange with neutral oxygen presents the largest barrier, and because of the higher thermal O^+ densities, this process can control the total O^+ escape flux into the magnetosphere.

At low field-aligned curent density or low scale height for the O^+ ion distribution, the escape flow decreases with increasing ionospheric density. As the field aligned current is increased the critical height for the instability is reduced, raising the total number of O^+ ion subjected to ion cyclotron heating and hence increasing the escape flow. Above a certain value the escape flow increases with ionospheric density, however, unless the O^+ is very large, the transition occurs at field-aligned current densitites greater than normally observed.

In steady state the total outflow is limited by the frictional drag on thermal O^+ ions, below the critical height, exerted by the neutral thermosphere. The escape outflow will only fall below this limit if the field-aligned current is low. Increased exospheric temperature will also tend to decrease the flow, as will high ionospheric density at low O^+ scale heights or low density with large scale heights.

APPENDIX A Evolution of Ion Pitch Angle θ for Adiabatic Motion in the Absence of Collisions

The net force on a transversely accelerated ion along the magnetic field line is the sum of the mirror and gravitational terms

$$F_\parallel = F_z = -\frac{E_\perp}{B}\frac{dB}{dz} - m_i g(r) \sin I \qquad (A1)$$

For a magnetic field $B = B_o (r/r_o)^3$, as used by Moore [1980] and Lysak et al. [1980], the field-aligned acceleration at r of an ion transversely accelerated to an energy $E_{\perp 0}$ at r_o (where the gravitational acceleration is g_o) is

$$\frac{dv_\parallel}{dt} = \sin I \left\{ \frac{3E_{\perp 0}\, r_o^{\,3}}{m_i\, r^4} - \frac{g_o\, r_o^{\,2}}{r^2} \right\} \qquad (A2)$$

By integration, the field-aligned velocity $V_\parallel$ is given by

$$v_\parallel^{\,2} = \frac{2E_{\parallel 0}}{m_i} + \frac{2E_{\perp 0}}{m_i}\left\{1 - \left(\frac{r_o}{r}\right)^3\right\} - \frac{2E_e}{m_i}\left\{1 - \frac{r_o}{r}\right\} \qquad (A3)$$

where $E_{\parallel 0}$ is the initial parallel kinetic energy at r_o; E_e is the gravitational escape energy required to remove the ion to infinite r and is given by

$$E_e = m_i g_o r_o = \frac{m_i g_s R_E^{\,2}}{r_o} \qquad (A4)$$

where $g = g_s$ at $r = R_E$. By conservation of energy

$$v^2 = \frac{2}{m_i}\left\{ E_{\parallel 0} + E_{\perp 0} - E_e\left(1 - \frac{r_o}{r}\right)\right\} \qquad (A5)$$

From equations (A3) and (A5)

$$\cos\Theta = \frac{v_\parallel}{v} = [1 + Z]^{-1/2}$$

where

$$Z = 1 + \frac{(r_o/r)^3}{\left(\frac{E_{\parallel 0}}{E_{\perp 0}}\right) + 1 - \left(\frac{r_o}{r}\right)^3 - \left(\frac{E_e}{E_{\perp 0}}\right)\left(1 - \frac{r_o}{r}\right)}$$

APPENDIX B The Number of Collisions Between a TAI and Neutral Thermospheric Atoms

Consider a hypothetical, transversely accelerated ion that is unaffected by ion-neutral interactions. In a small time, dt, it suffers dC such collisions with neutral atoms. If δ is the relative ion-neutral velocity, σ the collision cross section and N_n the density of neutral atoms then

$$dC = \sigma N_n \delta\, dt \qquad (B1)$$

The number occurring in a range of geocentric distance dr is

$$dC = \sigma N_n \frac{\alpha}{\sin I}\frac{v}{v_\parallel}\, dr \qquad (B2)$$

where I is the geomagnetic dip, v is the ion velocity, and $v_\parallel$ its field-aligned component; using the rms value for δ and a Maxwellian distribution of atomic velocities, α is given by

$$\alpha = \left\{1 + \left(\frac{3k\,T_n}{2e\,E_i}\right)\frac{m_i}{m_n}\right\} \qquad (B3)$$

where T_n is the neutral (exospheric) temperature, E_i is the ion's kinetic energy (in eV), m_i and m_n are the masses of the ion and atoms, respectively, k is boltzmann's constant, and e is the electronic charge. For an O^+ ion of energy 7-12 eV in a neutral O gas of temperature 750-1400K, α equals unity to within 1%. However, for such an ion in hydrogen gas of these temperatures, α varies between 1.06 and 1.14.

A parameter C is defined as the number of collisions an ion conic would suffer in moving between geocentric distances r_o and r_t if the ion were unaffected by each collision. Hence

$$C = \int_{r_o}^{r_t} \sigma N_n \frac{\alpha}{\sin I} \frac{dr}{\cos\theta} \qquad (B4)$$

and is therefore a measure of the "thickness" of the neutral atmospheric barrier presented to the ion. For adiabatic motion of the ion, the pitch angle θ and kinetic energy would evolve according to the equations given in appendix A. Substituting from equations (B3), (A5), and (A6) and asuming diffusive equilibrium of the thermospheric neutral gas, equation (B4) gives

$$C = N_{no} \int_{r_o}^{r_t} \frac{\sigma}{\sin I} \exp\left\{\frac{m_n g_o r_o}{kT_n}\left(\frac{r_o}{r} - 1\right)\right\}$$

$$\left\{1 + \frac{1}{\left[1 + \left(\frac{r}{r_o}\right)^3 \Delta\right]}\right\}\left\{1 + \frac{3k\, T_n\, m_i}{2_e\, m_n\, E_{\perp 0}\, \Delta}\right\} dr \qquad (B5)$$

where

$$\Delta = \frac{E_{\parallel 0}}{E_{\perp 0}} + 1 + \left(\frac{E_e}{E_{\perp 0}}\right)\left(1 - \frac{r_o}{r}\right)$$

and N_{no} is the neutral density at r_o.

Acknowledgements. The author is indebted to J E Titheridge for help in analyzing the thermal ion flow data. He is also grateful to the Auckland University Council for the award of a post doctoral research fellowship.

The Editor thanks E Ungstrup and another referee for their assistance in evaluating this paper.

References

Ashour-Abdalla, M., H. Okuda, and C. Z. Cheng, Acceleration of heavy ions on auroral field lines, Geophys. Res. Lett., 8, 795-798, 1981.

Balsiger, A., P. Eberhardt, J. Geiss, and D. T. Young, Magnetic storm injection of 0.9 to 16 keV/e solar and terrestrial ions into the high-altitude magnetosphere, J. Geophys. Res., 85, 1645-1662, 1980.

Bame, S. J., J. R. Ashbridge, A. J. Hundhausen, and M. D. Montgomery, Solar wind ions $^{58}Fe^{8+}$ to $^{56}Fe^{12+}$, $^{28}Si^{7+}$, $^{28}Si^{8+}$, and $^{16}O^{6+}$, J. Geophys. Res., 75, 6360-6365, 1970.

Banks, P. M. , Collision frequencies and energy transfer, Planet. Space Sci., 14, 1105-1122, 1966.

Banks, P. M., and G. Kockarts, Aeronomy, part A, Academic, New York, 1973.

Bohmer, H., and S. Fornaca, Experiments on nonlinear effects of strong ion cyclotron wave turbulence, J. Geophys, Res., 84, 5234-5240, 1979.

Bohmer, H., S. Fornaca, N. Rynn, and M. Wickham, Ion fluctuations and velocity distribution in the presence of ion cyclotron waves, Phys. Fluids, 21, 2208-2210, 1978.

Candidi, M., S. Orsini, and V. Formisano, The properties of ionospheric O^+ ions as observed in the magnetotail boundary layer and northern plasma lobe, J. Geophys. Res., 87, 9097-9106, 1982.

Cattell, C., The relationship of field-aligned currents to electrostatic ion cyclotron waves, J. Geophys. Res., 86, 3641-3645, 1981.

Chappell, C. R., Initial observations of thermal plasma composition and energetics from Dynamics Explorer 1, Geophys. Res. Lett. 9, 929-932, 1982.

Chappell, C. R., J. L. Green, J. F. E. Johnson, and J. H. Wait, Jr., Pitch angle variations in magnetospheric thermal plasma-initial observations from Dynamics Explorer 1, Geophys. Res. Lett. 9(9), 933-936, 1982.

Collin, H. L., R. D. Sharp, E. G. Shelley, and R. G. Johnson, Some general characteristics of upflowing ion beams over the auroral zone and their relationship to auroral electrons, J. Geophys. Res., 86, 6820-6826, 1981.

Cowley, S. W. H., Plasma populations in a simple open model magnetosphere, Space Sci. Rev., 26, 217-277, 1980.

Dakin, D. R., T. Tajima, G. Benford, and N. Rynn, Ion heating by the electrostatic ion cyclotron instability: theory and experiment, J. Plasma Phys., 15, 175-195, 1976.

Dum, C. T., and T. H. Dupree, Non linear stabilisation of high frequency instabilities in a magnetic field, Phys. Fluids, 13, 2064-2081, 1970.

Dusenbery, P. B. and L. R. Lyons, Generation of ion-conic distribution by upgoing ionospheric electrons, J. Geophys. Res., 86, 7627-7638, 1981.

Formisano, V., S. Orsini, and M. Candidi, Observation of ionospheric oxygen in the geomagnetic tail by ISEE 2, Adv. Space Res., 1, 313-318, 1981.

Frank, L. A., K. L. Ackerson, and D. N. Yeager, Observations of atomic oxygen (O^+) in the Earth's magnetotail, J. Geophys. Res., 82, 129-134, 1977.

Freeman, J. W., H. K. Hills, T. W. Hill, and P. H. Reiff, Heavy ion circulation in the Earth's magnetosphere, Geophys. Res. Lett., 4, 195-197, 1977.

Ghielmetti, A. C., R. G. Johnson, R. D. Sharp, and E. G. Shelley, The latitudinal, diurnal, and altitudinal distributions of upward flowing energetic ions of ionospheric

origin, Geophys. Res. Lett., 5, 59-62, 1978.

Gorney, D. J., A. Clarke, D.Croley, J.Fennell, J.Luhmann, and P. Mizera, The distribution of ion beams and conics below 8000 km, J. Geophys. Res., 86, 83-89, 1981.

Gurgiolo, C. and J. L. Burch, DE-1 observations of the polar wind - a heated and an unheated component, Geophys. Res. Lett., 9, 945-948, 1982.

Hauck, J. P., H. Bohmer, N. Rynn, and G. Benford, Ion beam excitation of ion cyclotron waves and ion heating in plasmas with drifting electrons, J. Plasma Physics, 19, 253-265, 1978.

Hedin, A. E., C. A. Reber, N. W. Spencer, H. C. Brinton, and D. C. Kayser, Global model of longitude/UT variations in thermospheric composition and temperature based on mass spectrometer data, J. Geophys. Res., 84, 1-9, 1979.

Horwitz, J. L., The ionosphere as a source for magnetospheric ions, Rev. Geophys. Space Phys., 20, 929-952, 1982.

Horwitz, J. L., C. R. Baugher, C. R. Chappell, E. G. Shelley, D. T. Young, and R. R. Anderson, ISEE 1 observations of thermal plasma in the vicinity of the plasmasphere during periods of quieting magnetic activity, J. Geophys. Res., 86, 9989-10001, 1981.

Horwitz, J. L., C. R. Baugher, C. R. Chappell, E. G. Shelley, and D. T. Young, Conical pitch angle distributions of very low-energy ion fluxes observed by ISEE 1, J. Geophys. Res., 87, 2311-2320, 1982.

Hudson, M. K., R. L. Lysak, and F. S. Mozer, Magnetic field-aligned potential drops due to electrostatic ion cyclotron turbulence, Geophys. Res. Lett., 5, 143-146, 1978.

Hultqvist, B., Recent progress in the understanding of the ion composition in the magnetosphere and some major question marks, Rev. Geophys. Space Phys., 20, 589-611, 1982a.

Hultqvist, B., On the origin of the hot ions in the disturbed dayside magnetosphere, preprint 056, Kiruna Geophys. Inst., Kiruna, Sweden, 1982.

Ionson, J. A., R. S. B. Ong, and E. G. Fontheim, Turbulent transport and heating in the auroral plasma of the topside ionosphere, Planet. Space Sci., 27, 203-210, 1979.

Johnson, R. G., Energetic ion composition in the Earth's magnetosphere, Rev. Geophys. Space Phys., 17, 696-705, 1979.

Kaye, S. M., E. G. Shelley, R. D. Sharp, and R. G. Johnson, Ion composition of zipper events, J. Geophys. Res., 86, 3383-3388, 1981.

Kindel, J. M., and C. F. Kennel, Topside current instabilities, J. Geophys. Res., 76, 3055-3078, 1971.

Kinter, P. M., M. C. Kelley, R. D. Sharp, A. G. Ghielmetti, M.Temerin, C. Cattell, P. F. Mizera, and J. F. Fennell, Simultaneous observations of energetic (keV) upstreaming and electrostatic hydrogen cyclotron waves, J. Geophys. Res., 84, 7201-7212, 1979.

Klumpar, D. M., Transversely accelerated ions: an ionospheric source of hot magnetospheric ions, J. Geophys. Res., 84, 4229-4237, 1979.

Klumpar, D. M., Transversely accelerated ions in auroral arcs, in Physics of auroral arc formation, Geophys. Monogr. Ser., vol. 25, edited by S. I. Akasofu and J. R. Kan, pp. 122-128, AGU, Washington, D C., 1981.

Knopf, H., E. A. Mason, and J. T. Vanderslice, Interaction energies, charge exchange cross sections and diffusion cross sections for N^+ and N^- or O^+ and O^- collisions, J. Chem. Phys. 40, 3548-3553, 1964.

Lee, K. F., Ion cyclotron instability in current carrying plasmas with anisotropic temperatures, J. Plasma Phys. 8, 379-386, 1972.

Lockwood, M., Thermal ion flows in the topside auroral ionosphere and the effects of low-altitude, transverse acceleration, Planet. Space Sci., 30, 595-609, 1982.

Lockwood, M., Field-aligned plasma flow in the quiet, mid-latitude ionosphere deduced from topside soundings, J. Atmos. Terr. Phys., 45, 1-14, 1983.

Lockwood, M., and J. E. Titheridge, Ionospheric origin of magnetospheric O^+ ions, Geophys. Res. Lett., 8, 381-384, 1981.

Lockwood, M., and J. E. Titheridge, Departures from diffusive equilibrium in the topside F-layer from satellite soundings, J. Atmos. Terr. Phys., 44, 425-440, 1982.

Lundin, R., B. Hultqvist, N. Pissarenko, and A. Zackarov, The plasma mantle: composition and other characteristics observed by means of the Prognoz-7 satellite, Space Sci. Rev., 31, 247-345, 1982a.

Lundin, R., B. Hultqvist, E. Dubinin, A. Zackarov, and N. Pissarenko, Observations of outflowing ion beams on auroral field lines of altitudes of many earth radii, Planet. Space Sci., 30, 715-726, 1982b.

Lyons, L. R., and T. E. Moore, Effects of charge exchange on the distribution of ionospheric ions trapped in the radiation belts near synchronous orbit, J. Geophys. Res., 86, 5885-5888, 1981.

Lysak, R. L., M. K. Hudson, and M. Temerin, Ion heating by strong electrostatic ion cyclotron turbulence, J. Geophys. Res., 85, 678-686, 1980.

Moore, T. E., Modulation of terrestrial escape flux composition (by low-altitude acceleration and charge exchange chemistry), J. Geophys. Res., 85, 2011-2116, 1980.

Mozer, F. S., C. Cattell, M. K. Hudson, R. L. Lysak, M. Temerin, and R. B. Torbert, Satellite measurements and theories of low altitude auroral particle acceleration, Space Sci. Rev., 27, 155-213, 1980.

Okuda, H., and M. Ashour-Abdalla, Formation of conical distribution and intense ion heating in the presence of hydrogen cyclotron waves, Geophys. Res. Lett., 8, 811-814, 1981.

Papadopoulos, K., J. D. Gaffey, Jr, and P. J. Palmadesso, Stochastic acceleration of large M/Q ions by hydrogen cyclotron waves in the magnetosphere, Geophys. Res. Lett.,7, 1014-1018, 1980.

Peterson, W. K., R. D. Sharp, E. G. Shelley, and R. G. Johnson, Energetic ion composition of the plasma sheet, J. Geophys. Res., 86, 761-767, 1981.

Peterson, W. K., E. G. Shelley, G. Haerendel, and G. Paschmann, Energetic ion composition in the subsolar magnetopause and boundary layer, J. Geophys. Res., 87, 2139-2145, 1982.

Prange, R., Energetic (keV) ions of ionospheric origin in the magnetosphere: A review, Ann. Geophys., 34, 187-214, 1978.

Pritchett, P. L., M. Ashour-Abdalla, and J. M. Dawson, Simulation of the current-driven electrostatic ion cyclotron instability, Geophys. Res. Lett., 8, 611-614, 1981.

Rynn, N., D. R. Dakin, D. L. Correll, and G. Benford, Ion heating by the current-driven electrostatic ion-cyclotron instability, Phys. Rev. Lett., 33, 765-768, 1974.

Sharp, R. D., D. L. Carr, W. K. Peterson, and E. G. Shelley, Ion streams in the magnetotail, J. Geophys. Res., 86, 4639-4648, 1981.

Shelley, E. G., A. G. Ghielmetti, and J. Geiss, The Polar Ionosphere as a source of energetic magnetospheric plasma, Geophys. Res. Lett. 9, 941-944, 1982.

Singh, N., and R. W. Schunk, Numerical calculations relevant to the initial expansion of the polar wind, J Geophys. Res., 87, 9154-9170, 1982.

Stern, R. A., D. L. Correll, H. Bohmer, and N. Rynn, Nonlocal effects in the electrostatic ion cyclotron instability, Phys. Rev. Lett., 37, 833-836, 1976.

Torr, M. R., and D. G. Torr, Energetic oxygen: a direct coupling mechanism between the magnetosphere and the thermosphere, Geophys. Res. Lett., 6, 700-702, 1979.

Torr, M. R., J. C. G. Walker, and D. G. Torr, Escape of fast oxygen from the atmosphere during geomagnetic storms, J. Geophys. Res., 79, 5267-5271, 1974.

Ungstrup, E., D. M. Klumpar, and W. J. Heikkila, Heating of ions to superthermal energies in the topside ionosphere by electrostatic ion cyclotron waves, J. Geophys. Res., 84, 4289-4296, 1979.

Whalen, B. A., W. Bernstein, and P. W. Daly, Low altitude acceleration of ionospheric ions, Geophys. Res. Lett., 5, 55-59, 1978.

Yau, A. W., B. A. Whalen, A. G. McNamara, P. J. Kellog, and W. Bernstein, Particle and wave observations of low-altitude ion acceleration events, J. Geophys. Res., 88, 341-355, 1983.

Young, D. T., H. Balsiger, and J. Geiss, Observed increase in the abundance of kilovolt O^+ in the magnetosphere due to solar cycle effects, Adv. Space Res., 1, 309-312, 1981.

Young, D. T., H. Balsiger, and J. Geiss, Correlations of Magnetospheric ion composition with geomagnetic and solar activity, J. Geophys. Res., 87, 9077-9096, 1982.

M. Lockwood, Rutherford Appleton Laboratory
Chilton, Didcot, Oxfordshire, OX11 0QX, England

(Received October 20, 1982;
revised July 26, 1983;
accepted July 29, 1983.)